Calculations for nuclear matter and finite nuclei within and beyond energy-density-functional theories through interactions guided by effective

Letter

Calculations for nuclear matter and finite nuclei within and beyond energy-density-functional theories through interactions guided by effective field theory

C. J. Yang [1,2] W. G. Jiang [1] S. Burrello [3] and M. Grasso [4]

[1]*Department of Physics, Chalmers University of Technology, SE-412 96 Göteborg, Sweden*
[2]*Nuclear Physics Institute of the Czech Academy of Sciences, 25069 Řež, Czech Republic*
[3]*Institut für Kernphysik, Technische Universität Darmstadt, 64289 Darmstadt, Germany*
[4]*Université Paris-Saclay, CNRS/IN2P3, IJCLab, 91405 Orsay, France*

(Received 4 October 2021; accepted 24 June 2022; published 21 July 2022)

We propose a novel idea to construct an effective interaction under energy-density-functional (EDF) theories which is adaptive to the enlargement of the model space. Guided by effective field theory principles, iterations of interactions as well as enlargements of the model space through particle-hole excitations are carried out for infinite nuclear matter and selected closed-shell nuclei (^{4}He, ^{16}O, ^{40}Ca, ^{56}Ni, and ^{100}Sn) up to next-to-leading order. Our approach provides a new way for handling the nuclear matter and finite nuclei within the same scheme, with advantages from both EDF and *ab initio* approaches.

DOI: 10.1103/PhysRevC.106.L011305

Introduction. One important challenge in the nuclear many-body problem concerns the construction of interactions. Existing state-of-the-art approaches can be mainly categorized into two extremes: one starts with bare nucleon-nucleon (NN) degrees of freedom and improves the results order by order following effective field theory (EFT) [1–14] through *ab initio* calculations [15–24]; the other adopts the energy-density-functional (EDF) framework to build an "in medium" interaction within the self-consistent mean-field (MF) approximation. However, both approaches suffer from long-standing shortcomings.

Indeed, although *ab initio* approaches allow one to construct the interaction on a clear foundation, they still suffer from technical difficulties concerning the reduction of the enormous model space required to converge the many-body calculations [25–37]. Attempts along this direction have been carried out through methods of unitary transformations [35–37] or an EFT procedure which accounts for both ultraviolet and infrared truncations [25–33]. Moreover, much effort has been spent to face theoretical problems related to the power counting issues [38–41] and the growing importance of three- and four-nucleon forces with the number of particles in the system [42–44]. Nonetheless, a definite solution to these questions is far from being assured.

On the other hand, a strong model dependence characterizes the effective interactions usually employed in the EDF framework, as derived at the MF level. To complicate matters, it is known that beyond-MF (BMF) effects need also to be taken into account. In contrast to the nonperturbative treatment adopted in *ab initio* calculations, approaches such as the MF Hartree-Fock approximation or BMF methods are then applied (see for instance Refs. [45–54]). However, BMF effects are usually evaluated by employing the same interaction fitted at MF, which generates an overcounting of correlations at the BMF level. More refined methods exist to overcome this problem, such as self-energy-subtraction procedures, which are used for example in the second random-phase approximation [45]. Nevertheless, there is a lack of an order-by-order organization scheme to generate effective interactions applicable to both nuclear matter and finite nuclei. Even more importantly, as a common drawback of both EDF and *ab initio* approaches, the interaction is defined in a fixed model space, which stays *unchanged* throughout all considered orders.

Inspired by recent efforts toward bridging EDF and EFT ideas [55–88], we probe in this work a novel possibility, which proposes to improve *both* the interaction and the model space order by order. Specifically, we assume there is an underlying EFT expansion where the MF results correspond to the leading-order (LO) contribution. Subleading corrections are then added, which contain the iterated LO interaction renormalized in an enlarged model space through particle-hole excitations. Constructing an EFT in this direction naturally leads to a novel setup which demands that

(1) The interaction must be adaptive to the growth of the model space at each order.
(2) Iterations of LO interactions must be performed through an in-medium propagator.

This strategy was already applied to infinite matter for instance in Refs. [58,62,65,75]. Note that an attempt to include the second-order Dyson diagrams has been proposed and

applied to the calculation of the ^{16}O binding energy in Ref. [89]. However, an investigation that fully exploits the advantages of an enlarged model space and analyzes the renormalizability of various power-counting scenarios for both nuclear matter and finite nuclei is so far absent.

We present here a first study where we apply such a strategy to both matter and finite nuclei, sertting the basis for a novel approach to be adopted in nuclear structure calculations. Our focus is indeed to develop a unified framework together with an order-by-order improvable and renormalizable interaction which has the potential to be applied to infinite nuclear matter and nuclei across the entire nuclear chart, as traditional EDF does.

Leading order. We start by defining the Hamiltonian $H_{\rm LO}$, which contains the kinetic term plus the LO interaction term $V^{\rm LO}$,

$$H_{\rm LO} = \sum_i e_i \hat{n}_i + \sum_{i>j} V_{ij}^{\rm LO}, \tag{1}$$

where e_i and $\hat{n}_i$ are the energy and the particle-number operator for the particle i. The interaction term $V_{ij}^{\rm LO}$ is a two-body operator to be determined. To speculate about a reasonable LO interaction under EDF, we make use of one basic requirement of EFT: the renormalizability of the observables. Studies performed for nuclear matter in Refs. [60,61,75] suggest that a t_0-t_3 model of Skyrme-type interactions is most likely to be a suitable candidate for $V^{\rm LO}$. MF calculations of Eq. (1) are straightforward for both nuclear matter and finite nuclei.

However, we do not adopt the conventional Hartree-Fock procedure here. Guided by empirical information (such as the information obtained by shell-model calculations fitted to experiments), one could start with an ansatz of the wave function Ψ and evaluate $H_{\rm LO}$ by calculating its matrix element. Note that here Ψ defines our model space at LO and does not change with the effective interaction. Reference [90] showed that reasonably good results can be obtained by directly evaluating the Gogny interaction between Ψ consisting of a single-particle basis constructed in the shell model. Inspired by that, we directly define our LO model space as the shell-model wave function up to the highest occupied shell and calculate the expectation value of the Hamiltonian perturbatively. The ground-state (g.s.) energy of the system at LO can be written as $E_{g.s.}^{\rm LO} = E_v + E_{\rm coul} - t_{CM} + E_c$, with $E_v, E_{\rm coul}, E_c$ the energies of valence particles, the Coulomb potential, and the core contributions, respectively; $t_{CM} = \frac{3}{4}\hbar\omega$ is the center-of-mass (CM) kinetic energy. Throughout this exploratory work we only consider closed-shell nuclei, so that $E_v = 0$, and the Coulomb potential is treated within the mean-field approximation. The core energy can be further written as the core kinetic energy plus the core potential energy, that is $E_c = t_c + V_c$, where [90]

$$V_c = \sum_{j_a^c \leqslant j_b^c} \sum_{JT} (2T+1)(2J+1)\langle j_a^c j_b^c JT | V^{\rm LO} | j_a^c j_b^c JT \rangle,$$
$$t_c = \sum_{j_a^c} (2T+1)(2J+1)\langle j_a^c | \hat{t} | j_a^c \rangle. \tag{2}$$

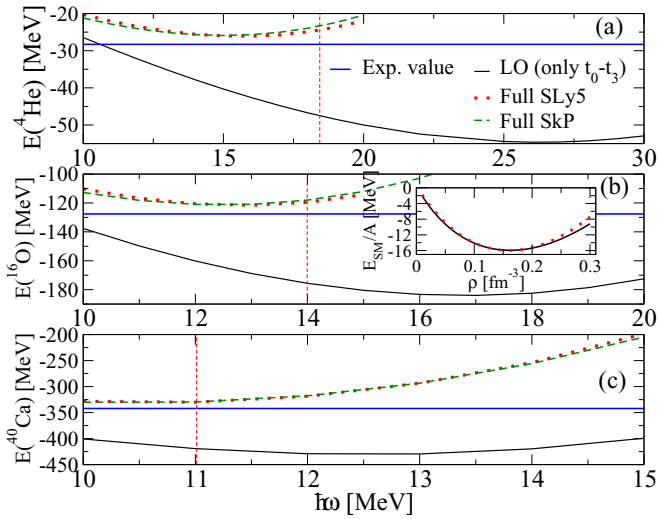

FIG. 1. Ground state energies of ^{4}He (a), ^{16}O (b), and ^{40}Ca (c) as a function of $\hbar\omega$. Results obtained from a t_0-t_3 model and full SLy5 and SkP functionals are plotted as black solid, red dotted, and green dashed lines, respectively. The empirical $\hbar\omega$ value for each nucleus is marked as a red vertical dashed line. The horizontal blue lines represent the experimental energies. The SM energy per particle at LO is plotted as a function of the density ρ in the inset.

Here j_a^c, j_b^c label the single-particle orbits in the core, $\hat{t}$ is the kinetic energy operator, and J and T are the total angular momentum and isospin quantum numbers for each pair of interacting particles, respectively.

Note that the combination of the harmonic oscillator (HO) strength $\hbar\omega$ and $N_{\rm max}$ (denoting the truncation up to the highest occupied shell) provides a natural cutoff of the Fermi sphere in finite nuclei and might play a similar role as the Fermi momentum k_F in the nuclear matter case. Since our interaction is singular, without additional regulators, results in general will not converge with the increase of $\hbar\omega$. For each nucleus, there exists an optimal $\hbar\omega$ so that the shell-model basis matches the size of the nucleus. For nuclei with mass number A, the empirical value $\hbar\omega \approx 45A^{-1/3} - 25A^{-2/3}$ is frequently adopted [91]. With the above equations, evaluations of the g.s. energies of ^{4}He, ^{16}O and ^{40}Ca using $V^{\rm LO}$ are straightforward. The detailed derivation is given in Refs. [89,90] and summarized in the Supplemental Material [92], together with the form assumed by the adopted LO interaction.

We present the g.s. energies as a function of $\hbar\omega$ in Fig. 1, where a t_0-t_3 model of the SkP parametrization [93] is adopted for $V^{\rm LO}$. LO calculations systematically provide strongly overbound nuclei with respect to experimental data, even at the empirical value of $\hbar\omega$, though the corresponding MF equation of state (EoS) for symmetric matter (SM) (shown in the inset of Fig. 1) is quite satisfactory. This is not surprising judging from the simple form of the LO interaction. We have tried other t_0-t_3 parametrizations, which reproduce as well the empirical SM EoS, and found that the systematic overbinding persists. On the other hand, with the $t_{1,2}$ Skyrme terms included, the MF g.s. energies obtained from SkP [93] or SLy5 [94,95] are very reasonable, with the minimum also located

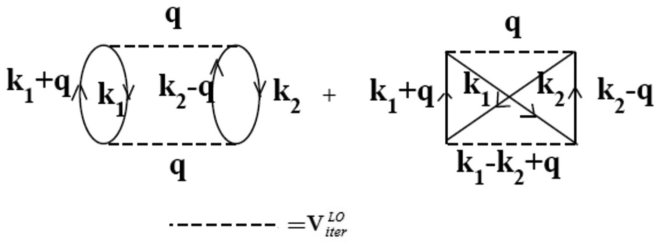

FIG. 2. Once-iterated diagrams for the interaction $V_{\rm iter}^{\rm LO}$. $\mathbf{k}_1$ ($\mathbf{k}_2$) denotes the single-particle momentum of the initial (final) state, and $\mathbf{q}$ is the transferred momentum.

close to the empirical $\hbar\omega$ value. Although an EFT should aim to capture the most important physics already at LO, one could argue that basic physics is roughly captured once the equation of state of symmetric matter can be reproduced up to saturation density.

Next-to-leading order: Two possibilities of improvements. To improve further, two approaches are possible. First, one could add more terms to the effective interaction together with an EFT-based speculation on their form or importance, and then evaluate again Eq. (1) to produce better fits to a wider range of nuclear properties. Many attempts have been devoted in this direction [69–73,96–98]. On the other hand, since nuclei are bound states, they should be generated by at least partial iteration of a certain interaction. The MF description might be then improved by considering higher-order corrections coming from the iterated diagrams, such as the ones corresponding to the enlargement of the model space through particle-hole excitations. Improvements in this direction are much less studied, as iterating effective interactions built at MF level in the loops usually generates self-consistency problems, unless renormalization is taken care of properly.

Starting from next-to-leading order (NLO), we improve our theory by considering both of the above directions, and demonstrate how to establish self-consistent NLO corrections through proper renormalization procedures. Up to NLO, one has

$$E_{\rm NLO} = E^{\rm LO} + \langle\Psi|V_{ij}^{CT}|\Psi\rangle + E_{\rm iter}^{\rm NLO}, \tag{3}$$

where V_{ij}^{CT} is the higher-order contact interaction entering at NLO with its contribution evaluated at the MF level [the same way as in Eq. (2)]. The structure of V_{ij}^{CT} has to be determined according to the renormalizability and the power-counting scheme. $E_{\rm iter}^{\rm NLO}$ represents the contribution of the once-iterated diagrams shown in Fig. 2. The general form of $E_{\rm iter}^{\rm NLO}$ reads [99]

$$E_{\rm iter}^{\rm NLO} = -\frac{1}{4}\sum_{j_a^c\leqslant j_b^c, X_\alpha\leqslant X_\beta}\frac{|\langle j_a^c j_b^c JT|V_{\rm iter}^{\rm LO}|X_\alpha X_\beta JT\rangle|^2}{\varepsilon_\alpha+\varepsilon_\beta-\varepsilon_a-\varepsilon_b}, \tag{4}$$

where $j_{a(b)}^c$ are the same as in Eq. (2) because one stops at the highest occupied orbital; $X_{\alpha(\beta)}$ stands for excited states, where the summation starts at the Fermi sphere and stops at an upper limit which defines the second-order model space; $\varepsilon_i = k_i^2/2m$ is the single-particle energy of each state having momentum k_i (the effective mass is set to its bare value $m =$ 939 MeV in this work). $V_{\rm iter}^{\rm LO}$ denotes the part of the LO interaction which is iterated to provide the NLO contribution. A straightforward evaluation of Eq. (4) is in principle possible. However, the truncation applied to the excited states in the single-particle basis cannot be directly matched with the truncation performed for the EoS of matter in Refs. [60,61,75], where a relative momentum cutoff Λ is applied. Moreover, Moshinsky transformations require all excited states $X_{\alpha,\beta}$ to be represented in terms of the HO basis,[1] which complicates the matching between different nuclei, as they correspond to different $\hbar\omega$ and $X_{\alpha(\beta)}$.

To produce a renormalized interaction to be easily applied to all cases, we proceed as follows. First, since excitations are governed by $V_{\rm iter}^{\rm LO}$, one can directly represent the relevant wave functions in relative coordinates. Let us call $\mathbf{k}_1$, $\mathbf{k}_2$ ($\mathbf{k}_1'$, $\mathbf{k}_2'$) the single-particle momenta of the initial/final (intermediate) state. Then, the incoming and outgoing momenta in relative coordinates are $\mathbf{k} = (\mathbf{k}_1 - \mathbf{k}_2)/2$, $\mathbf{k}' = (\mathbf{k}_1' - \mathbf{k}_2')/2 + \mathbf{q}$, where $\mathbf{q}$ is the transferred momentum. Equation (4) can be rewritten as

$$E_{\rm iter}^{\rm NLO} = \frac{f(\hbar\omega)}{4}\left[\int d^3\mathbf{k}\int d^3\mathbf{k}'\int d^3\mathbf{K}\langle\Psi(\mathbf{K};\mathbf{k})|V_{\rm iter}^{\rm LO}(\mathbf{k};\mathbf{k}')|\psi(\mathbf{k}')\rangle G\langle\psi(\mathbf{k}')|V_{\rm iter}^{\rm LO}(\mathbf{k}';\mathbf{k})|\Psi(\mathbf{K};\mathbf{k})\rangle\right]_{BC}, \tag{5}$$

where

$$G = \frac{-m}{k'^2 - k^2}. \tag{6}$$

Ψ is represented in the same basis used at LO, which depends on the CM momentum $\mathbf{K} = \mathbf{k}_1 + \mathbf{k}_2 = \mathbf{k}_1' + \mathbf{k}_2'$ and on the relative momentum $\mathbf{k}$. $\psi = \sum_i \phi_i$ denotes the intermediate excitations, where ϕ_i can be represented by any complete basis. One caveat is that if one chooses to expand Ψ and ψ in a different basis, an overall factor $f \neq 1$ will be needed to fix the norm. To define the intermediate model space, one must truncate it either by the number of basis states or by the highest momentum. In this work, we choose the second option and adopt the free wave-packets basis so that f depends only on $\hbar\omega$. The detailed derivation leading to Eq. (5) is given in the Supplemental Materials [92]. Note that the conversion of initial/final and intermediate single-particle-basis states (which are also restricted as mentioned before) to relative coordinates results in a boundary condition (BC) which couples k_F to new variables $\mathbf{k}$, $\mathbf{k}'$, and $\mathbf{K}$. The threefold integration under the same BC has been carried out to obtain the second-order EoS [62,99], and is to be carried out in a similar manner in

[1] Alternatively, one could go through extra processes which involve the decomposition of the chosen basis into the HO one [100,101].

TABLE I. k_A (in fm^{-1}) for ^{4}He, ^{16}O and ^{40}Ca under various $\hbar\omega$. Those adopted in Fig. 3 are highlighted by bold text.

$\hbar\omega$ (MeV)	11	12	13	14	15	16	17	18
k_A of ^{4}He	0.90	0.95	0.98	1.02	1.05	1.08	**1.12**	1.15
k_A of ^{16}O	1.08	1.13	1.18	**1.22**	1.26	1.30	1.34	1.38
k_A of ^{40}Ca	**1.25**	1.37	1.35	1.40	1.45	1.49	1.54	1.58

Eq. (5). However, unlike the nuclear matter case—where a clear definition of Fermi momentum is possible—k_F is not clearly given in finite nuclei. In the nuclear matter case, the radial integral dk is truncated by $k \in [0, k_F]$. On the other side, in finite nuclei, the same integrals are carried out through $k \in [0, \infty]$. However, the shell structure (the LO wave functions of a nucleus at a chosen $\hbar\omega$) provides a natural truncation analogous to k_F. To proceed, we interpret k_F in finite nuclei to be the highest momentum each wave function can access. The procedure to extract k_F in a finite nucleus is thus the following. First, we evaluate the g.s. energy at the MF level and separate the contributions from the t_0, the t_3, and the V^{CT} terms for each nucleus. Then, we compare the ratios $\frac{\langle t_0\rangle}{\langle t_3\rangle}$ and $\frac{\langle t_0\rangle}{\langle V^{CT}\rangle}$ to their corresponding values in SM. The ratios in nuclear matter depend on k_F, whereas the same ratios in finite nuclei are related to their shell structure. By requiring the same ratios between finite nuclei and nuclear matter, we can extract the corresponding k_F for ^{4}He, ^{16}O, and ^{40}Ca (denoted as k_A) under various $\hbar\omega$ values. The resulting k_A are listed in Table I. One can see that a heavier nucleus (and a larger $\hbar\omega$) naturally corresponds to a higher k_A. We have tried several interactions having different values of α (the power of the density in the t_3 term) and found a very weak spreading ($\leqslant$1% variations for $\alpha \approx 0.16$–0.3)[2] between the values of k_A obtained by using such interactions in the matching of the ratios.

Once k_A is known, we have all the ingredients to perform actual calculations. In Refs. [61,75], the full t_0-t_3 LO interaction is iterated to generate $E^{\rm NLO}_{\rm iter}$ for nuclear matter. The same procedure can be performed in principle in Eq. (5) for finite nuclei. However, some conceptual subtleties arise regarding how to account for the density ρ when one considers the fluctuation of the wave functions due to the intermediate excitations. In fact, in conventional EDF approaches with a density-dependent term included (for example the t_3 term of Skyrme interactions), the interaction does not correspond to a genuine Hamiltonian. The iteration of this term generates a conceptual drawback and may lead to technical problems such as divergences in BMF calculations for nuclei [102–104]. Also, the density-dependent term depends on the wave function and this could potentially complicate an EFT analysis. Therefore, we choose not to iterate the t_3 part of the interaction in this work.

In the following, we perform two types of NLO calculations:

(1) Only the t_0 part of the LO interaction is iterated, and $V^{CT} = C(1 + x_c P_\sigma)$.

[2]For α up to 1, the extracted k_F can vary up to 5%.

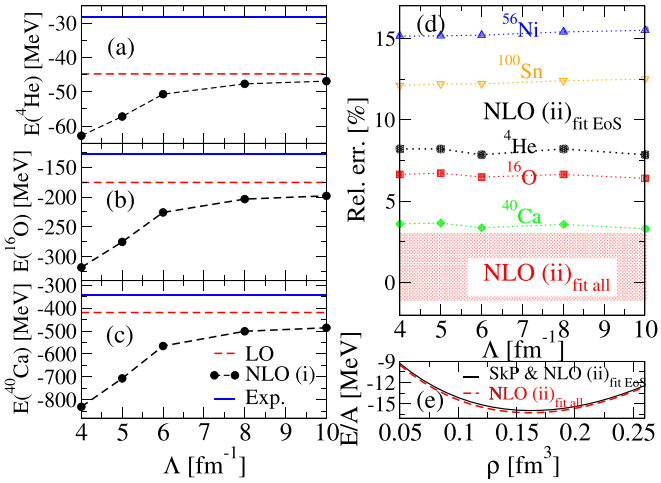

FIG. 3. Left panels (a)–(c): Ground state energies up to NLO for ^{4}He, ^{16}O, and ^{40}Ca as a function of Λ. Right panel (d): Rel. err. $= (E_b - E_{\rm exp.})/|E_{\rm exp.}|$ for the first five closed-shell, $N = Z$ nuclei. The labels NLO (i) and NLO (ii) refer to the two prescriptions described in the main text, where parameters in NLO (ii) are obtained by either fitting to EoS only (fit EoS) or an overall fit including EoS and all five nuclei (fit all). Their corresponding EoSs are plotted in (e).

(2) Same as (i), but with additional $V^{CT}_{ii} = \frac{1}{2}t_1(1 + x_1 P_\sigma)(\mathbf{k}'^2 + \mathbf{k}^2) + t_2(1 + x_2 P_\sigma)\mathbf{k}' \cdot \mathbf{k}$, that is, the Skyrme-type $t_{1,2}$ terms are added.

Note that the above interactions are Skyrme-like, and $P_\sigma = (1 + \sigma_1\sigma_2)/2$ is the spin-exchange operator. We treat C, x_c, α, $t_{0,1,2,3}$, and $x_{0,1,2,3}$ as the low-energy constants (LECs) in EFT, and we choose to renormalize them to reproduce the SLy5 SM and neutron matter (NM) EoSs. The LECs, the χ^2 values and the resulting EoSs are given in the Supplemental Material [92]. Predictions on g.s. energies of ^{4}He, ^{16}O, ^{40}Ca, ^{56}Ni, and ^{100}Sn evaluated up to NLO with $\Lambda = 4$–10 fm^{-1}, are given in Fig. 3, where the empirical $\hbar\omega = 45A^{-1/3} - 25A^{-2/3}$ are adopted. As one can see, the pathological overbinding trend at LO seems to persist under the prescription (i). Thus, without the entrance of new k_F dependencies in the EoS (other than terms that behave asymptotically $\sim k_F^4$ and proportional to t_0^2) at NLO, one does not observe any improvement from LO to NLO for the EoSs of both matter and finite nuclei. Nevertheless, the NLO renormalizability is satisfied, which is reflected in the converging pattern of NLO (i) results against Λ. A real improvement is achieved by the prescription (ii), where, by just fitting to the empirical EoSs, reasonable reproductions of the experimental binding $E_{\rm exp.}$ are found for nuclei up to mass number $A = 40$ (with |relative error| $= \frac{|E_b - E_{\rm exp.}|}{|E_{\rm exp.}|} \leqslant 8\%$, where E_b is the resulting binding energy). This suggests that the t_1, t_2 terms are indeed indispensable, as indicated by many phenomenological studies. However, the error grows to $\sim$15% when extending the calculation to the next two $N = Z$ nuclei (^{56}Ni and ^{100}Sn). Note that the curves labeled as NLO (ii)$_{\rm fit\ EoS}$ are obtained by keeping the original SkP or SLy5 values of $t_{1,2,3}$, $x_{1,2,3}$, and α, while adjusting only t_0, C, and

$x_{0,c}$ to two EoSs.[3] Up to NLO, the computational cost stays very closed to the MF calculations and is relatively small. Thus, we attempt a second fit (utilizing all LECs but keeping $\alpha = 1/6$) to the empirical EoSs and all five nuclei. We found it is possible to reproduce the experimental binding for all five nuclei within 3% [denoted by the red shaded area and labeled as NLO $(\text{ii})_{\text{fit all}}$ in Fig. 3], if one allows the SM EoS to be slightly ($\leqslant$2%) more attractive around saturation than the one produced by SkP [panel (e), Fig. 3].

Power counting: Particle-number-dependent high- and low-momentum scales. Finally, we speculate about the high- and low-momentum scales M_{hi} and M_{lo} in our EFT expansion. Since M_{lo} spans from 0 to k_F—which varies with A in a nucleus—a successful EFT arrangement of observables up to NLO in terms of powers series in (M_{lo}/M_{hi}) suggests that M_{hi} has the following properties:

(1) It is at least larger than k_F, and depends on the number of particles A.
(2) It depends on $N_{\max}$ and $\hbar\omega$, at least for those nuclei where central densities are lower than the saturation density of SM. Let us denote by A_s typical A values for which nuclei reach the saturation density in their central region. Then M_{hi} increases with A for $A < A_s$.

The breakdown scale has a functional form $M_{hi}(A, \hbar\omega)$. For $A < A_s$, the asymptotic form of the EFT expansion is $\frac{M_{lo}}{M_{hi}} \sim \frac{k}{\beta k_F(A)}$, where k is the characteristic center-of-mass momentum scale and $\beta \gtrapprox 1$. On the other hand, $\beta k_F(A) \sim \bar{M}_{hi}$, that is, it becomes a constant for $A > A_s$, where $\bar{M}_{hi}$ is a hard breakdown scale to be extracted by a Lepage-like plot [105,106] from NLO and next-to-next-to-leading order (NNLO) results; $\frac{2}{3\pi^2}\bar{M}_{hi}^3$ and $\frac{1}{3\pi^2}\bar{M}_{hi}^3$ correspond to the highest density ρ for which one can trust the EoS of SM and NM, respectively (for example, twice the saturation density of SM).

Summary. In summary, we provide a novel framework to include BMF correlations order by order. With a reliable extraction of k_F, the treatment of finite nuclei and nuclear matter can be performed on the same footing. Investigations up to NLO are performed for five $N = Z$ closed-shell nuclei and for nuclear matter for the first time. We have tested various arrangements of NLO corrections through renormalization-group analysis. Note that our analysis are based on a trial-and-error procedure. Since not all possibilities are tested, our NLO prescription (ii) might still be subjected to further refinements. Nevertheless, the trial-and-error procedure carried out in present work—which checks the renormalizability of the in-medium loops (and therefore the self-consistency of the proposed beyond mean field corrections)—can be repeated with different interactions in the future. Thus, our work serves as a starting point toward an EFT-based description of nuclei across the entire nuclear chart. Many interesting future works including the treatment of higher-order correlations and a full EFT power-counting analysis are in progress.

Acknowledgments. This work was supported by the Czech Science Foundation GACR Grants No. 19-19640S and No. 22-14497S, the Swedish Research Council (Grant No. 2017-04234), the European Research Council (ERC) under the European Union's Horizon 2020 research and innovation program (Grant Agreement No. 758027). Computational resources were supplied by the project "e-Infrastruktura CZ" (e-INFRA CZ LM2018140) supported by the Ministry of Education, Youth and Sports of the Czech Republic, IT4Innovations at Czech National Supercomputing Center under Project No. OPEN-24-21 1892, the Swedish National Infrastructure for Computing (SNIC) at Chalmers Centre for Computational Science and Engineering (C3SE), and the National Supercomputer Centre (NSC) partially funded by the Swedish Research Council. S.B. acknowledges support from the Alexander von Humboldt Foundation.

[3]LECs adjusted to SkP and SLy5 EoSs produce $\leqslant 1\%$ difference in E_b up to ^{40}Ca, and are indistinguishable in Fig. 3.

[1] S. Weinberg, Phys. Lett. B **251**, 288 (1990).
[2] S. Weinberg, Nucl. Phys. B **363**, 3 (1991).
[3] C. Ordóñez, L. Ray, and U. van Kolck, Phys. Rev. Lett. **72**, 1982 (1994).
[4] C. Ordóñez, L. Ray, and U. van Kolck, Phys. Rev. C **53**, 2086 (1996).
[5] E. Epelbaoum, W. Glöckle, and U.-G. Meissner, Nucl. Phys. A **637**, 107 (1998).
[6] E. Epelbaum, W. Glöckle, and U.-G. Meissner, Nucl. Phys. A **671**, 295 (2000).
[7] D. Entem and R. Machleidt, Phys. Lett. B **524**, 93 (2002).
[8] D. R. Entem and R. Machleidt, Phys. Rev. C **66**, 014002 (2002).
[9] E. Epelbaum, W. Glöckle, and U.-G. Meissner, Nucl. Phys. A **747**, 362 (2005).
[10] E. Epelbaum, H. Krebs, and U. G. Meißner, Eur. Phys. J. A **51**, 53 (2015).
[11] U. V. Kolck, Prog. Part. Nucl. Phys. **43**, 337 (1999).
[12] P. F. Bedaque and U. V. Kolck, Annu. Rev. Nucl. Part. Sci. **52**, 339 (2002).
[13] E. Epelbaum, H.-W. Hammer, and U.-G. Meissner, Rev. Mod. Phys. **81**, 1773 (2009).
[14] H.-W. Hammer, S. König, and U. van Kolck, Rev. Mod. Phys. **92**, 025004 (2020).
[15] W. H. Dickhoff and C. Barbieri, Prog. Part. Nucl. Phys. **52**, 377 (2004).
[16] D. Lee, Prog. Part. Nucl. Phys. **63**, 117 (2009).
[17] S. K. Bogner, R. J. Furnstahl, and A. Schwenk, Prog. Part. Nucl. Phys. **65**, 94 (2010).
[18] B. R. Barrett, P. Navrátil, and J. P. Vary, Prog. Part. Nucl. Phys. **69**, 131 (2013).
[19] A. Carbone, A. Cipollone, C. Barbieri, A. Rios, and A. Polls, Phys. Rev. C **88**, 054326 (2013).
[20] G. Hagen, T. Papenbrock, M. Hjorth-Jensen, and D. J. Dean, Rep. Prog. Phys. **77**, 096302 (2014).
[21] H. Hergert, S. Bogner, T. Morris, A. Schwenk, and K. Tsukiyama, Phys. Rep. **621**, 165 (2016).
[22] J. Carlson, S. Gandolfi, F. Pederiva, S. C. Pieper, R. Schiavilla, K. E. Schmidt, and R. B. Wiringa, Rev. Mod. Phys. **87**, 1067 (2015).

[23] N. Barnea, W. Leidemann, and G. Orlandini, Nucl. Phys. A **650**, 427 (1999).
[24] W. Glöckle, H. Witala, D. Hüber, H. Kamada, and J. Golak, Phys. Rep. **274**, 107 (1996).
[25] I. Stetcu, B. R. Barrett, P. Navrátil, and J. P. Vary, Phys. Rev. C **71**, 044325 (2005).
[26] I. Stetcu, B. R. Barrett, and U. van Kolck, Phys. Lett. B **653**, 358 (2007).
[27] I. Stetcu, B. R. Barrett, U. van Kolck, and J. P. Vary, Phys. Rev. A **76**, 063613 (2007).
[28] I. Stetcu, J. Rotureau, B. R. Barrett, and U. van Kolck, J. Phys. G: Nucl. Part. Phys. **37**, 064033 (2010).
[29] J. Rotureau, I. Stetcu, B. R. Barrett, M. C. Birse, and U. van Kolck, Phys. Rev. A **82**, 032711 (2010).
[30] I. Stetcu, J. Rotureau, B. R. Barrett, and U. van Kolck, Ann. Phys. (NY) **325**, 1644 (2010).
[31] J. Rotureau, I. Stetcu, B. R. Barrett, and U. van Kolck, Phys. Rev. C **85**, 034003 (2012).
[32] S. Binder, A. Ekström, G. Hagen, T. Papenbrock, and K. A. Wendt, Phys. Rev. C **93**, 044332 (2016).
[33] X. Zhang, S. R. Stroberg, P. Navrátil, C. Gwak, J. A. Melendez, R. J. Furnstahl, and J. D. Holt, Phys. Rev. Lett. **125**, 112503 (2020).
[34] C.-J. Yang, Phys. Rev. C **94**, 064004 (2016).
[35] R. Roth, A. Calci, J. Langhammer, and S. Binder, Phys. Rev. C **90**, 024325 (2014).
[36] S. K. Bogner, T. T. S. Kuo, and A. Schwenk, Phys. Rep. **386**, 1 (2003).
[37] S. K. Bogner, R. J. Furnstahl, and R. J. Perry, Phys. Rev. C **75**, 061001(R) (2007).
[38] U. van Kolck, Front. Phys. **8**, 79 (2020).
[39] E. Epelbaum and J. Gegelia, Eur. Phys. J. A **41**, 341 (2009).
[40] H. W. Griesshammer, Few-Body Syst. **63**, 44 (2022).
[41] U. van Kolck, Few-Body Syst. **62**, 85 (2021).
[42] C. J. Yang, A. Ekström, C. Forssén, and G. Hagen, Phys. Rev. C **103**, 054304 (2021).
[43] C. J. Yang, Eur. Phys. J. A **56**, 96 (2020).
[44] C. J. Yang, A. Ekström, C. Forssén, G. Hagen, G. Rupak, and U. van Kolck, arXiv:2109.13303.
[45] D. Gambacurta, M. Grasso, and J. Engel, Phys. Rev. C **92**, 034303 (2015).
[46] D. Gambacurta, M. Grasso, and J. Engel, Phys. Rev. Lett. **125**, 212501 (2020).
[47] C. Robin and E. Litvinova, Phys. Rev. C **98**, 051301(R) (2018).
[48] C. Robin and E. Litvinova, Phys. Rev. Lett. **123**, 202501 (2019).
[49] Y. F. Niu, G. Colò, and E. Vigezzi, Phys. Rev. C **90**, 054328 (2014).
[50] G. Colò, P. F. Bortignon, M. Brenna, X. Roca-Maza, E. Vigezzi, K. Moghrabi, M. Grasso, and K. Mizuyama, Phys. Scr. **89**, 054006 (2014).
[51] G. Colò, H. Sagawa, and P. F. Bortignon, Phys. Rev. C **82**, 064307 (2010).
[52] S. Burrello, J. Bonnard, and M. Grasso, Phys. Rev. C **103**, 064317 (2021).
[53] S. Burrello, M. Colonna, G. Colò, D. Lacroix, X. Roca-Maza, G. Scamps, and H. Zheng, Phys. Rev. C **99**, 054314 (2019).
[54] S. Burrello, M. Colonna, and H. Zheng, Front. Physi. **7**, 53 (2019).
[55] H. Hammer and R. Furnstahl, Nucl. Phys. A **678**, 277 (2000).
[56] N. Kaiser, J. Phys. G: Nucl. Part. Phys. **42**, 095111 (2015).
[57] N. Kaiser, Eur. Phys. J. A **53**, 104 (2017).
[58] K. Moghrabi, M. Grasso, G. Colo, and N. Van Giai, Phys. Rev. Lett. **105**, 262501 (2010).
[59] K. Moghrabi, arXiv:1607.05829.
[60] C. J. Yang, M. Grasso, K. Moghrabi, and U. van Kolck, Phys. Rev. C **95**, 054325 (2017).
[61] C. Yang, M. Grasso, and D. Lacroix, Phys. Rev. C **94**, 031301(R) (2016).
[62] C. J. Yang, M. Grasso, X. Roca-Maza, G. Colò, and K. Moghrabi, Phys. Rev. C **94**, 034311 (2016).
[63] D. Lacroix, A. Boulet, M. Grasso, and C.-J. Yang, Phys. Rev. C **95**, 054306 (2017).
[64] M. Grasso, D. Lacroix, and C. J. Yang, Phys. Rev. C **95**, 054327 (2017).
[65] C. J. Yang, M. Grasso, and D. Lacroix, Phys. Rev. C **96**, 034318 (2017).
[66] J. Bonnard, M. Grasso, and D. Lacroix, Phys. Rev. C **101**, 064319 (2020).
[67] M. Grasso, Prog. Part. Nucl. Phys. **106**, 256 (2019).
[68] J. Bonnard, M. Grasso, and D. Lacroix, Phys. Rev. C **98**, 034319 (2018).
[69] H. Gil, P. Papakonstantinou, C. H. Hyun, T.-S. Park, and Y. Oh, Acta Phys. Pol. B **48**, 305 (2017).
[70] H. Gil*, Y. Oh, C. H. Hyun, and P. Papakonstantinou, New Phys.: Sae Mulli **67**, 456 (2017).
[71] H. Gil, P. Papakonstantinou, C. H. Hyun, and Y. Oh, JPS Conf. Proc. **20**, 011041 (2018).
[72] H. Gil, Y.-M. Kim, C. H. Hyun, P. Papakonstantinou, and Y. Oh, Phys. Rev. C **100**, 014312 (2019).
[73] H. Gil, Y.-M. Kim, P. Papakonstantinou, and C. Ho, Phys. Rev. C **103**, 034330 (2021).
[74] R. J. Furnstahl, Eur. Phys. J. A **56**, 85 (2020).
[75] S. Burrello, M. Grasso, and C.-J. Yang, Phys. Lett. B **811**, 135938 (2020).
[76] F. Marino, C. Barbieri, A. Carbone, G. Colò, A. Lovato, F. Pederiva, X. Roca-Maza, and E. Vigezzi, Phys. Rev. C **104**, 024315 (2021).
[77] G. De Gregorio, F. Knapp, N. Lo Iudice, and P. Veselý, Phys. Rev. C **105**, 024326 (2022).
[78] F. Andreozzi, F. Knapp, N. Lo Iudice, A. Porrino, and J. Kvasil, Phys. Rev. C **75**, 044312 (2007).
[79] F. Andreozzi, F. Knapp, N. Lo Iudice, A. Porrino, and J. Kvasil, Phys. Rev. C **78**, 054308 (2008).
[80] D. Bianco, F. Knapp, N. Lo Iudice, F. Andreozzi, and A. Porrino, Phys. Rev. C **85**, 014313 (2012).
[81] G. De Gregorio, F. Knapp, N. Lo Iudice, and P. Vesely, Phys. Rev. C **93**, 044314 (2016).
[82] G. De Gregorio, F. Knapp, N. Lo Iudice, and P. Vesely, Phys. Rev. C **94**, 061301(R) (2016).
[83] G. De Gregorio, F. Knapp, N. Lo Iudice, and P. Veselý, Phys. Rev. C **95**, 034327 (2017).
[84] G. D. Gregorio, F. Knapp, N. L. Iudice, and P. Veselý, Phys. Scr. **92**, 074003 (2017).
[85] G. De Gregorio, F. Knapp, N. Lo Iudice, and P. Veselý, Phys. Rev. C **97**, 034311 (2018).
[86] G. De Gregorio, F. Knapp, N. Lo Iudice, and P. Veselý, Phys. Rev. C **99**, 014316 (2019).
[87] G. De Gregorio, F. Knapp, N. Lo Iudice, and P. Veselý, Phys. Rev. C **101**, 024308 (2020).

[88] G. De Gregorio, F. Knapp, N. Lo Iudice, and P. Veselý, Phys. Lett. B **821**, 136636 (2021).
[89] M. Brenna, G. Colò, and X. Roca-Maza, Phys. Rev. C **90**, 044316 (2014).
[90] W. G. Jiang, B. S. Hu, Z. H. Sun, and F. R. Xu, Phys. Rev. C **98**, 044320 (2018).
[91] J. Blomqvist and A. Molinari, Nucl. Phys. A **106**, 545 (1968).
[92] See Supplemental Material at http://link.aps.org/supplemental/10.1103/PhysRevC.106.L011305 for a detailed derivation of the formulas given in main text and the parameters used to obtain the results.
[93] J. Dobaczewski, H. Flocard, and J. Treiner, Nucl. Phys. A **422**, 103 (1984).
[94] E. Chabanat, P. Bonche, P. Haensel, J. Meyer, and R. Schaeffer, Nucl. Phys. A **627**, 710 (1997).
[95] E. Chabanat, P. Bonche, P. Haensel, J. Meyer, and R. Schaeffer, Nucl. Phys. A **635**, 231 (1998); **643**, 441(E) (1998).
[96] P. Becker, D. Davesne, J. Meyer, J. Navarro, and A. Pastore, Phys. Rev. C **96**, 044330 (2017).
[97] K. Bennaceur, A. Idini, J. Dobaczewski, P. Dobaczewski, M. Kortelainen, and F. Raimondi, J. Phys. G: Nucl. Part. Phys. **44**, 045106 (2017).
[98] D. Davesne, J. Navarro, J. Meyer, K. Bennaceur, and A. Pastore, Phys. Rev. C **97**, 044304 (2018).
[99] K. Davies and M. Baranger, Nucl. Phys. A **120**, 254 (1968).
[100] G. Papadimitriou, B. R. Barrett, J. Rotureau, N. Michel, and M. Płoszajczak, EPJ Web Conf. **66**, 02006 (2014).
[101] G. Papadimitriou, J. Rotureau, N. Michel, M. Płoszajczak, and B. R. Barrett, Phys. Rev. C **88**, 044318 (2013).
[102] D. Lacroix, T. Duguet, and M. Bender, Phys. Rev. C **79**, 044318 (2009).
[103] M. Bender, T. Duguet, and D. Lacroix, Phys. Rev. C **79**, 044319 (2009).
[104] T. Duguet, M. Bender, K. Bennaceur, D. Lacroix, and T. Lesinski, Phys. Rev. C **79**, 044320 (2009).
[105] H. W. Grießhammer, *in 8th International Workshop on Chiral Dynamics (CD), Pisa, Italy, June 29–July 3* [PoS **CD15**, 104 (2015)].
[106] H. W. Grießhammer, Eur. Phys. J. A **56**, 118 (2020).